A hybrid electrochemical flow reactor to couple H 2 oxidation to NADH regeneration for biochemical reactions

Wassim El Housseini, François Lapicque, Alain Walcarius, Mathieu Etienne

A hybrid electrochemical flow reactor to couple H_2 oxidation to NADH regeneration for biochemical reactions

Wassim El Housseini[a,b] , François Lapicque[b], Alain Walcarius[a], Mathieu Etienne[a,*]

[a] *CNRS and Université de Lorraine, LCPME, UMR7564, 405 rue de Vandoeuvre, F-54600 Villers-lès-Nancy, France*

[b] *CNRS and Université de Lorraine, LRGP, UMR7274, ENSIC, BP 20451, F-54001 Nancy, France*

Abstract

Beta-nicotinamide adenine dinucleotide (NAD^+/NADH) is an important enzymatic co-factor that can be efficiently regenerated using a rhodium-based catalyst as electron transfer mediator (*i.e.* $[Cp^*Rh(bpy)Cl]^+$, where Cp* = pentamethylcyclopentadienyl and bpy = 2,2-bipyridine). Here, the above mediated regeneration of NADH is implemented in a redox flow bioreactor hybridized with a gas diffusion electrode for hydrogen oxidation. The reactor was initially optimized with respect to rhodium complex and NAD^+ concentrations, humidification of the hydrogen gas, flow rates of both H_2 gas and electrolytic solution, and solution pH. The integration of an enzymatic reaction consuming the generated NADH was then investigated in a flow process, combining in series the electrochemical reactor to a biochemical cell with immobilized L-lactic dehydrogenase for the conversion of pyruvate to lactate. A high activity was achieved with a turnover number up to 370 h^{-1} for NADH regeneration. Coupled electrochemical regeneration to enzymatic reaction led to total turnover number values of 2000 and $6.3*10^6$ for NADH electrochemical regeneration and bioconversion, respectively.

Keywords: β-nicotinamide adenine dinucleotide; $[Cp^*Rh(bpy)Cl]^+$; gas diffusion electrode; flow reactor; electrochemical regeneration

Correspondence: Dr. Mathieu Etienne (mathieu.etienne@univ-lorraine.fr)

1. Introduction

NAD^+/NADH cofactor and its phosphorylated derivative ($NADP^+$/NADPH) are important biological cofactors that play a critical role as electron shuttles in biological systems.[1] They can also be applied as an electron carrier in enzymatic systems catalyzing stereo- and regioselective reactions having a great biotechnological potential, *e.g.* dehydrogenases or cytochrome P450.[2] However, NADH and its derivatives in enzymatic systems are expensive,[a] so the regeneration of the enzymatically-active reduced form of the cofactor is strongly required.

Four methods for regeneration of the NAD(P)H cofactor can be employed: (i) chemical and photochemical regenerations, (ii) biological regeneration, (iii) enzymatic regeneration, (iv) electrochemical regeneration or electroenzymatic regeneration.[8] To quantify and compare the efficiency of each method, two criteria are usually defined: the turnover number (TN in h^{-1}) and the total turnover number (TTN). TN, which is homogeneous to a frequency, expresses the velocity at which the cofactor is regenerated. TTN provides information on the number of moles of product formed per mole of cofactor during the entire synthesis reaction of the targeted product.[2]

The average TTN of the enzymatic cofactor in the different regeneration methods has been reported to be in the order of 105 using chemical regeneration,[4] 21 with photochemical regeneration,[5] between 100 000 and 150 000 using enzymatic regeneration,[6–8] and between 101 and 3760 by electrochemical regeneration.[9–11] The difference between the TTN values obtained in enzymatic and electrochemical regenerations appears to be due to the nature of the

[a] NAD^+ 88.2 €/g, NADH 206 €/g, $NADP^+$ 355 €/g, NADPH 1330 €/g (A chemical provider catalog consulted the 12/12/2020)

catalytic reaction that is used, i.e. homogeneous versus heterogeneous, and of the mediator used in enzymatic and indirect electrochemical regenerations respectively.

A technique for the regeneration of NADH – or NADPH – cofactor must allow TTN larger than 1000 in order to be economically viable.[12,13] However, the technique that enables to reach the highest TN or TTN is not always the most economical due to the loss of the cofactor, or its thermal, chemical, or photochemical degradation.[13]

In fact, none of the regeneration methods cited above appear to offer a fully satisfactory solution to the problem of NADH regeneration that fulfils economic and environmental criteria for its application.[18] It is often reported that the cost of the technology or the products used for the regeneration of this cofactor (particularly enzymes used in enzymatic regeneration) are in the same order of magnitude or even higher than the cost of the cofactor and present problems related to their possible inhibition effects.[20] Therefore, TTN is not the only criterion for the economic evaluation of the process. The optimization of the reactor design, the limitation of the formation of by-products such as the inactive form of NADH, and the prevention of the NADH degradation during the process, all play an important role in the regeneration technique of NADH.[21]

The regeneration of NADH through electrochemical techniques is one of the most promising and controllable approaches that are used for the reduction of NAD^+.[2,22,23] It offers an easy separation of products of the reaction, if catalysts are immobilized, and it allows as well the control of the potential and the progress of the reaction.[24] The direct regeneration of NADH at bare electrodes only occurs at very negative potentials leading to the inactive dimerized form of NADH formed through one electron transfer instead of two electrons exchanged in the indirect regeneration of the NADH cofactor.[25] The usage of a mediator leads to the active form NADH

with a potential lower than the potential needed in the direct regeneration. $[Cp^*Rh(bpy)Cl]^+$ (chloro(2,2′-bipyridyl) (pentamethylcyclopentadienyl)-rhodium (III)) acting as a redox mediator has been shown to be the best non-enzymatic catalyst for the selective regeneration of NADH.[15,26,27]

The mechanism of NADH regeneration consists first in the reduction of the $[Cp^*Rh(bpy)Cl]^+$ **(M_{ox})** complex to [Cp*Rh(bpy)] **(M_{red1})** through two electron transfers,[28] which can be globally written as:

$$[\mathrm{Cp}*\mathrm{Rh(bpy)Cl}]^+ + 2\,e^- \rightleftharpoons [\mathrm{Cp}*\mathrm{Rh(bpy)}] + Cl^- \quad (1)$$

The reduced complex is protonated to rhodium hydride complex ($[Cp^*Rh(bpy)H]^+$, **M_{red2}**): [28]

$$[\mathrm{Cp}*\mathrm{Rh(bpy)}] + H^+ \rightleftharpoons [\mathrm{Cp}*\mathrm{Rh(bpy)H}]^+ \qquad k_2 = 10.6\ s^{-1}\ \text{at pH} = 7.5 \quad (2)$$

NAD^+ can then reduce to 1,4-NADH with the hydride form of the complex (**M_{red2}**) acting as a mediator:[29]

$$NAD^+ + [Cp*Rh(bpy)H]^+ + Cl^- \xrightarrow{k3} NADH + [Cp*Rh(bpy)Cl]^+ \quad (3)$$

Development of continuous flow reactors has occupied a wide range of interest by chemical engineers for over one decade due to their high efficiency when being compared with batch reactors.[30] In continuous flow reactors, reactants are continuously fed into the reactor and emerge as a continuous stream of products.[31] These continuous flow reactors are more and more used by chemists for the synthesis of fine chemicals such as NADH.[32] Electrochemical developments in continuous flow reactors have contributed to the reduction in energy consumption, to the improvement of material transport, and to increased conversion and selectivity[33] through more refined cell design and technology. It is anticipated that the synthesis

in flow will be coupled in the future with new analytical techniques for online monitoring of the process and speeding up the isolation and the purification.[34]

As shown in equations (2) and (3), the reactions are associated with proton transfer. The oxidation of hydrogen on platinum appears attractive for the generation of protons required at the biocathode for electrochemical synthesis offering the possibility to be applied as a reducing agent in a hybrid reactor combining a fuel cell and a redox flow device. This reaction is highly selective, producing no toxic or hazardous species.[35]

The electrochemical regeneration of fine chemicals, *e.g.* NADH, by indirect electrochemical reaction coupled with the oxidation of hydrogen is limited by the solubility of hydrogen in the electrolyte.[36] Gas diffusion electrodes (GDEs) have proven to boost current density by overcoming the poor solubility of hydrogen in aqueous electrolytes[37] and reducing gas-liquid mass transfer constraints.[37] Recently, GDEs have been applied to bioelectrochemical synthesis in continuous flow reactors[38,39] and evaluated for anodic NAD^+ regeneration coupled with energy production.[40]

While being compared to chemical catalysts, enzymes are known as efficient biocatalysts offering high competitive processes and becoming well recognized in organic synthesis and biotechnology.[41,42] The electrochemical regeneration of the NADH cofactor through a rhodium complex mediator can be coupled to a bioconversion for the synthesis of fine chemicals and to assess whether the regenerated NADH cofactor is in its active form.[24] Besides, for the sake of long term stability and reusability, enzymatic catalysts have to be immobilized[43] as for example by adsorption on carbon materials.[44]

In the present work, we combined the above approaches, namely the electrochemical regeneration of NADH mediated by a rhodium complex, the application of continuous flow reaction, and hydrogen oxidation using a GDE, in a single reactor with recirculation of the electrolytic solution. This approach relies upon the electrochemical reactor coupling efficiently the reduction of NAD^+ to the anode oxidation of hydrogen. The proposed process has been optimized by varying operating factors, *e.g.* the concentrations of rhodium complex and NAD^+, the pH, the activation procedure for the carbon-based electrode, as well as the cell operating conditions. Finally, the conversion of pyruvate to lactate by L-lactic dehydrogenase (LDH) has been carried out in the process after insertion of an enzymatic module in series with the electrochemical reactor, to check the activity of the in-situ regenerated NADH cofactor. The purpose of this study is to evaluate the contribution of this redox flow technology on the performance of NADH regeneration with a well described rhodium electrocatalyst.[15]

2. Materials and methods

2.1. Chemical and reagents

β-nicotinamide adenine dinucleotide (NAD^+, >98%) and β-nicotinamide adenine dinucleotide reduced dipotassium salt (NADH, >97%), K_2HPO_4 (99%), KH_2PO_4 (99%), HCl (37 %), Tris HCl (99 %), L-lactic dehydrogenase (LDH) from bovine heart (≥ 250 units/mg protein, 144,000 Da.), pyruvate (98 %) and lactate (98 %) were from Sigma-Aldrich. Phosphate buffer (0.1 M) was used to investigate the electrocatalytic properties of the rhodium complex towards NAD^+ reduction and was reported to be the most appropriate for such experiments[45]. Multiwall carbon nanotubes (MWCNT, NC7000™ series) were from Nanocyl (Belgium) and carbon papers (SpectraCarb 2050L-0550 Carbon Paper) were acquired from Fuel Cell Store (USA). MWCNT

were dispersed in a solution of ethanol (96 %). All solutions were prepared with high purity water (18 MΩ cm) from a Purelab Option water purification system.

2.2. Rhodium complex synthesis

$[Cp^*Rh(bpy)Cl]^+$ complex was prepared in a $CHCl_3$ solution after stoichiometric reaction between the 2,2-bipyridine and the pentamethylcyclopentadienyl rhodium(III) chloride dimer $(RhCp^*Cl_2)_2$. After addition of the reagents, the solution has been stirred for three hours under air and at room temperature then allowed to settle overnight at 8 °C. The solid complex was recovered by filtration by Buchner filtration.[24]

2.3. Electrode pretreatment

A piece of graphite felt (GFD4.6EA, SGL, Germany) being 4 cm x 4 cm x 0.4 cm in dimensions was used as cathode in the reactor (flow cell in Scheme 1). The as-received material is hydrophobic which can limit the good distribution of solution in the reactor. The graphite felt (GF) piece was treated to provide a suitable wettability using washing in successive solutions:[46] the GF piece was first immersed in ethanol and submitted to ultrasounds for 15 minutes at 25 °C, then, the process was repeated with 80:20, 60:40, 40:60 and 20:80 ethanol-water solutions and ending with pure water.

2.4. Enzymatic carbon paper with MWCNT (LDH-CP-MWCNT) preparation

A piece of SpectraCarb carbon paper being 1.5 cm x 1.5 cm x 0.05 cm was used as the enzyme support for the conversion of pyruvate to lactate using L-lactate dehydrogenase. The MWCNT-containing CP was prepared following the same process for a bucky paper electrode preparation reported in literature.[47] 10 mg MWCNT were dispersed in 50 mL ethanol by ultrasonication for 5 h. Afterwards, the suspension was decanted and vacuum filtered using the CP as filter. Then,

the material was dried at 60 °C overnight. This process has been repeated three times to obtain the desired number of MWCNT layers. Finally, an LDH enzyme was adsorbed on the MWCNT surface by depositing 50 µL suspension of LDH (500 units, *i.e.* 2 mg) and keeping for 2 hours at a temperature of 3°C.

2.5. Electrochemical reactor

Scheme 1 shows the electrochemical reactor used in this study. A Pt/C gas diffusion electrode (Paxitech France) with a Pt content at 0.2 $mg.cm^{-2}$, was used as anode and installed on a graphite bipolar plate, with grooved 1 x 1 mm^2 channels forming three channel clusters for continuous hydrogen introduction and distribution in the anode chamber. The gas diffusion electrode allows uniform and constant production rates of protons and electrons for a given flow rate of hydrogen. 40 mL of reaction solution, containing 0.1 M phosphate buffer and various amounts of NAD^+ and $[Cp^*Rh(bpy)Cl]^+$, were introduced to the glass storage tank. Temperature was at ambient level and unless specified otherwise, the initial pH was adjusted to 7.2. The solution was circulating continuously using a peristaltic pump through a graphite felt (4 cm x 4 cm x 0.4 cm), known as a good electrical conductor and acting as a three-dimensional cathode, with homogeneous distribution of the solution: this configuration is expected to be more efficient than a carbon foil as used in former works.[15] A Nafion membrane (N-212) was placed between the two electrodes for separation of the two compartments – in particular to avoid anode flooding from the solution treated at the cathode – and to permit a uniform proton transport rate from the anode to the cathode. Two copper ending plates allowed mechanical cohesion of the cell and electrical connection to the potentiostat (Bio-Logic VSP3). Continuous nitrogen bubbling was allowed in the storage tank using a sintered glass sparging system for saturating the gas with water at ambient temperature to avoid undesired evaporation of water during the NADH

production tests.[48] Both nitrogen and hydrogen flow rates were controlled by mass flowmeters (Brooks).

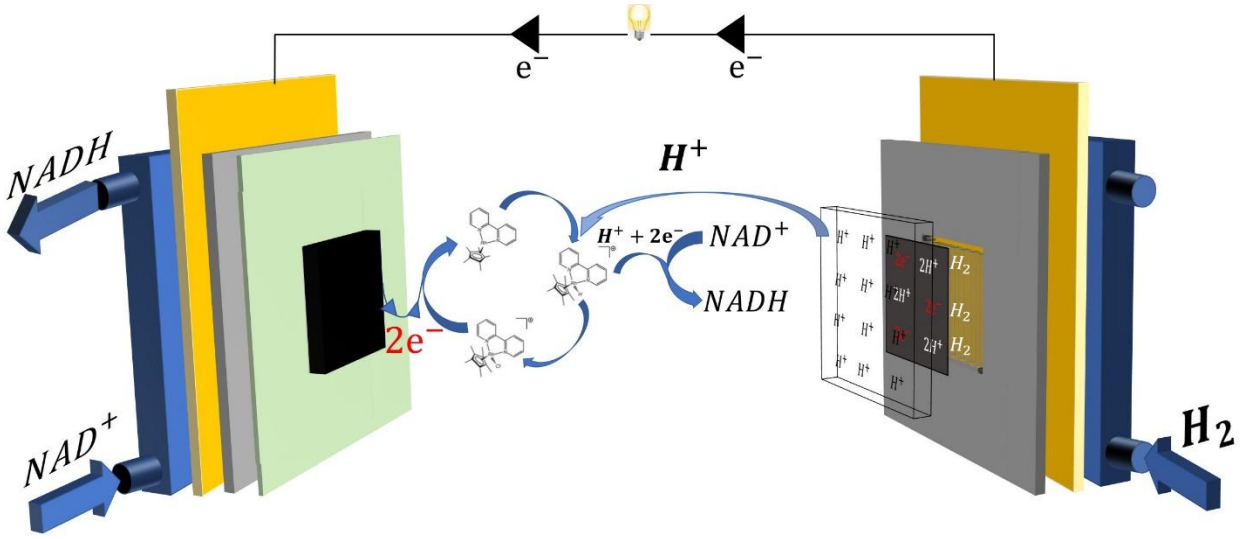

Scheme 1. Schematic view of the flow electrochemical reactor. Solution flow is on the left side and hydrogen flow is on the right side. A proton-conducting Nafion membrane is separating the gas diffusion electrode, for hydrogen oxidation, from the graphite felt electrode, for NADH production by electrocatalytic reduction of NAD^+ with $[Cp^*Rh(bpy)Cl]^+$ complex.

Cyclic voltammograms and batch electrolysis were performed in a two-electrode configuration, the hydrogen anode acting also as reference electrode. The usage of a two-electrode configuration where the anode acts as reference can be considered here because of the very low polarization of gas diffusion anode with current densities below 10 mA cm^{-2}. All potentials are thus given versus H^+/H_2 couple, noted ref. (H_2). Potential scan rate was fixed 5 mV s^{-1}. In electrolysis tests, the solution was sampled at regular intervals (each 5 or 10 minutes) and the conversion of NAD^+ to NADH was followed by UV absorption at 340 nm after suitable dilution (10 times). For the production of NADH, two protons are produced by hydrogen oxidation while one proton is consumed by NAD^+ reduction, according to the stoichiometry of both reactions. In

consequence, the pH slightly decreased during electrosynthesis, but owing to the buffer concentration, the pH change was never larger than 0.4 unit. The biological activity of the cofactor was then confirmed by reaction with a lactate dehydrogenase immobilized in the enzymatic cell.

2.6. Enzymatic cell

Scheme 2 shows the enzymatic cell used for the conversion of pyruvate to lactate connected in series with the electrochemical reactor (Scheme 1). The solution containing the rhodium complex, NADH, and the pyruvate was fed to the enzymatic cell through a graphite plate with grooved 1 x 1 mm^2 channels forming three channel clusters for its homogeneous distribution. The solution then percolated through a carbon felt that maintains the stability of the enzymes immobilized on the MWCNT-CP, which was put in contact with the felt. A gas diffusion layer, known as hydrophobic, has been placed in contact with the rear side of the LDH-MWCNT-CP preventing the adsorption of the solution, thus ensuring the stability of the enzymes even at high solution flow rates. The whole assembly was stacked between two polymeric (PMMA) plates for mechanical cohesion and to prevent solution leakage. The solution leaving the enzymatic cell with a higher lactate content, was pumped to the glass storage provided by N_2 degassing before returning to the electrochemical reactor. Samples taken at regular intervals were analyzed by HPLC using a Laminex separation column with 0.05 M H_2SO_4 as eluant.

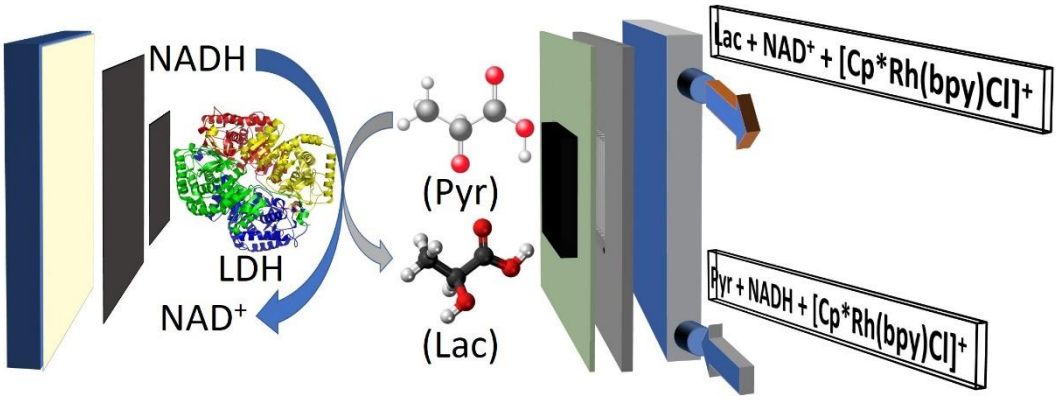

Scheme 2. Schematic view of the enzymatic cell. Solution flows from the right side.

3. Results and discussion

3.1. Evidence of electrochemical NADH Regeneration

The catalytic response of the GF electrode for the NADH regeneration was evaluated by cyclic voltammetry (Figure 1A). In the presence of 250 µM $[Cp^*Rh(bpy)Cl]^+$ (curve b), a redox signal is observed, showing a cathodic peak at -0.39 V and an anodic peak at -0.27 V. The intensity of the cathodic peak is approximately double that of the anodic peak. The latter corresponds to the oxidation of the reduced active form of the rhodium complex I ($[Cp^*Rh(bpy)H]^+$: M_{red2}). However, the first reduced form remains inactive ([Cp*Rh(bpy)]: M_{red1}) and unsuitable for redox reactions. Addition of 2.5 mM NAD^+ to the above solution (curve c) led to a large increase in the cathodic peak caused by the electrocatalytic reduction of NAD^+ by $[Cp^*Rh(bpy)H]^+$ and not by the direct reduction of NAD^+ which is observed at much cathodic potential values (and usually gives non-active forms of the cofactor, *i.e.* dimers).[25,49] The cathodic peak was observed at a potential slightly more negative (-0.45 V) than that observed with the reduction of the complex only. The cause of this potential shift can be a limitation associated to the electron transfer

kinetics on the graphite felt electrode[24] or to other ohmic losses in the configuration of the system.

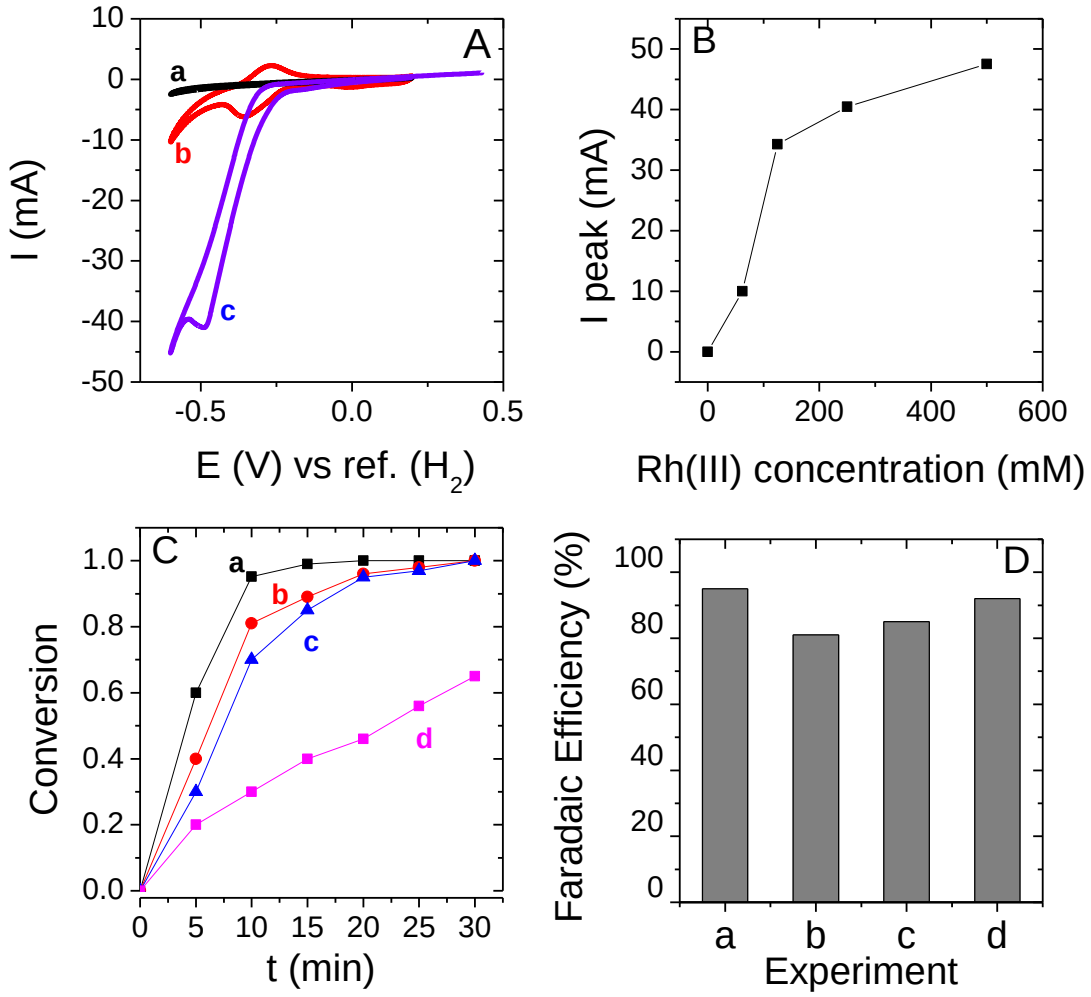

Figure 1. (A) Cyclic voltammograms recorded at 5 $mV.s^{-1}$ successively with the graphite felt electrode in (a) buffer solution (b) after addition of 250 µM $[Cp^*Rh(bpy)Cl]^+$ and (c) after addition of 2.5 mM NAD^+. (B) Influence of the rhodium complex concentration on the cathodic current peak measured by CV. (C and D) Influence of the catalyst concentration and the electrolysis potential on (C) the conversion rate of 2.5 mM NAD^+ to NADH and (D) the faradaic efficiency; (a) 62.5 µM $[Cp^*Rh(bpy)Cl]^+$ at -0.5 V vs ref. (H_2); (b) 250 µM $[Cp^*Rh(bpy)Cl]^+$ at -0.4 V vs ref. (H_2); (c) 125 µM $[Cp^*Rh(bpy)Cl]^+$ at -0.4 V vs ref. (H_2); (d) 62.5 µM $[Cp^*Rh(bpy)Cl]^+$ at -0.4 V vs ref. (H_2). All experiments were carried out in 0.1 M phosphate buffer solution at pH 7.2 under nitrogen atmosphere with a solution and hydrogen flow rates of 20 $mL.min^{-1}$ each.

The effect of the rhodium complex concentration on the intensity of the cathodic peak has been investigated at a fixed concentration of NAD^+ (2.5 mM); it shows that this intensity increases steeply with the mediator concentration before levelling off at higher concentrations (Figure 1B). The corresponding CV responses are presented in Figure S1 in Supporting Information.

The rhodium complex concentration and the cathode potential in electrolysis tests are important operating parameters that should be adjusted for optimizing the process of the regeneration of NADH. The performance of an electrochemical process is based on two criteria: conversion X measured by UV-visible absorption for NADH regeneration (Figure 1**C**), and the faradaic efficiency Φ expressing the fraction of electrons involved in the key electrochemical reaction (Figure 1**D**).

$$X = \frac{[NADH]_t}{[NAD^+]_0} \qquad \Phi = \frac{Q_{experimental}}{Q_{\ theorical}} = \frac{n_{e^-} \times F \times [NAD^+]_0 \times V \times X}{I \times t} \times 100 \qquad = \frac{7720 \times [NAD^+]_0 \times X}{I \times t} \times 100$$

;

n_{e^-} = 2; F=96500 C/mol; V = 40 mL

At -0.4 V vs ref. (H_2) and with an initial concentration of NAD^+ of 2.5 mM, the NADH was totally regenerated within 30 min for a rhodium complex concentration of 125 µM (curve c) and 250 µM (curve b). However, while decreasing the concentration of the rhodium complex to 62.5 µM, the conversion was limited to 0.62 after this lapse of time (curve d). At this potential, the faradaic efficiency is higher, attaining 92% by using the lowest concentration of the rhodium complex (62.5 µM) and 80 % with 250 µM of rhodium complex (see data b-d in Figure 1D). In order to increase the conversion with a rhodium complex concentration of 62.5 µM with 2.5 mM NAD^+, tests were made at -0.5 V vs ref. (H_2). Total conversion was observed within 20 min (see curve a in Figure 1C), with a faradaic efficiency of 96 % (data a in Figure 1D) which is actually

far larger than the values usually reported in the relevant literature in the range 50-70 %,[15] indicating the high selectivity and production rate of the process. Working at -0.5 V seems thus to be very promising based on the total conversion within an optimal time and the high faradaic efficiency. One explanation of these better performances can be found in Figure S1 of the Supporting Information (blue curve). The maximum cathodic current was observed around -0.5 V. Applying -0.5 V vs ref. (H_2), led thus to the highest conversion rate. On the contrary, applying -0.4 V vs ref. (H_2) led to a much lower current and consequently to a lower conversion rate. Note that the ratio between rhodium complex and NAD^+ was also found critical to reach complete conversion, as doubling the cofactor concentration to 5 mM with 62.5 µM $[Cp^*Rh(bpy)Cl]^+$ led to incomplete conversion (Figure S2 in Supporting Information). We suppose that a high concentration of NADH is hindering the catalytic activity of the rhodium catalyst for NAD^+ reduction. Actually, we do not know if this effect is reversible or irreversible. In any case, high concentration of cofactor is not meaningful for the electrosynthetis application ~~that is~~ targeted here.

Finally, to validate that the total regeneration of 2.5 mM of NADH was achieved in the presence of 62.5 µM of the rhodium complex and at a potential of -0.5 V vs ref, the biochemical conversion of 2.5 mM pyruvate to lactate was carried out in the presence of lactate dehydrogenase in the solution. Results are reported in Figure S3 of the Supporting Information, they show that indeed 2.5 mM lactate were produced within 200 min.

3.2. Optimization of hydrogen and solution flows

Flow of hydrogen in the anodic compartment and solution flow through the cathode chamber represent also important operating conditions in the electrochemical regeneration of NADH.

The used nitrogen was humidified as expressed above. In addition, it is noted that in operation of membrane fuel cells, the reacting gases are often humidified to improve the membrane conductivity and protons transport in the vicinity of the Pt clusters.[50] In consequence, the hydrogen used in first tests has been humidified as well.

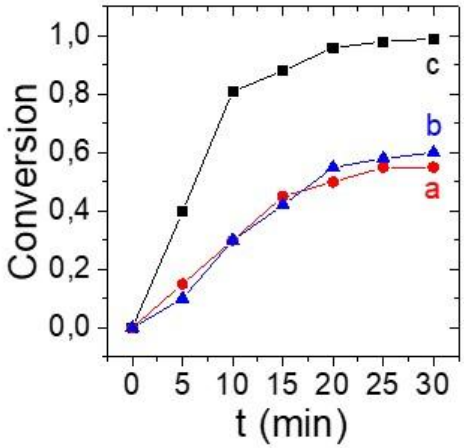

Figure 2. Influence of humidified hydrogen on the production of NADH at -0.4 V vs ref. (H_2) All experiments were done in 0.1 M phosphate buffer solution at pH 7.2 in the presence of 2.5 mM NAD^+ and 250 µM $[Cp^*Rh(bpy)Cl]^+$ under nitrogen atmosphere with a solution flow rate of 20 $mL.min^{-1}$ and (a) humidified hydrogen with a flow rate of 20 $mL.min^{-1}$, (b) humidified hydrogen with a flow rate of 10 $mL.min^{-1}$, (c) non-humidified hydrogen with a flow rate of 20 $mL.min^{-1}$.

Figure 2 shows the effect of hydrogen humidification on the conversion of 2.5 mM NAD^+ with 250 µM rhodium complex, at -0.4 V vs ref. (H_2). With humidified hydrogen, the conversion at room temperature, was observed to be limited to 0.55 and 0.50 with 10 (Figure 2, curve b**)** and 20 $mL.min^{-1}$ H_2 respectively (Figure 2, curve a) after 30 min conversion. Dismantling the cell and examination of its components showed that the GDE catalyst was soaked, thus not

suitable anymore for H_2 oxidation. With fully humidified hydrogen, the water activity in the ionomer becomes very large which may favor water flux from the (liquid phase) cathode medium, resulting in severe flooding of the anode.

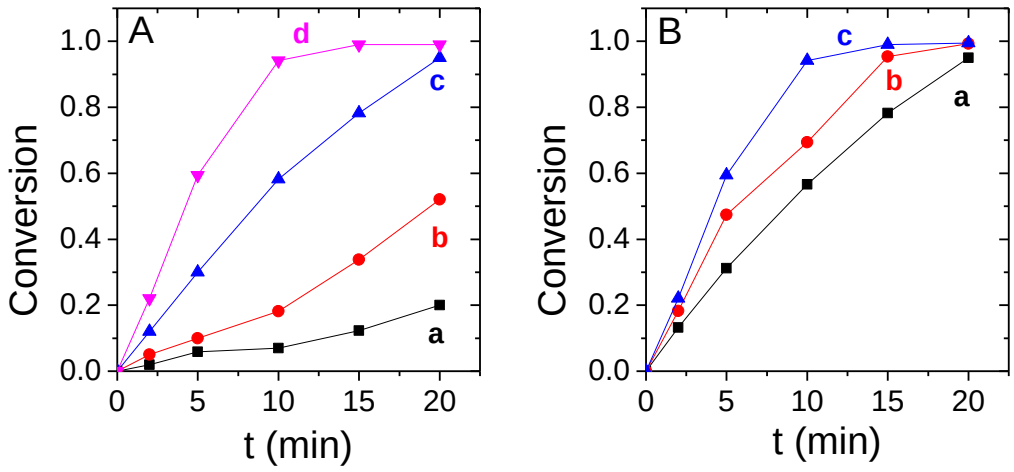

Figure 3. Influence of (A) hydrogen flow rate ((a) 1 (b) 5, (c) 10 and (d) 20 mL.min^{-1}) and (B) solution flow rate ((a) 4, (b) 10 and (c) 20 mL.min^{-1}) on the conversion of NAD^+. Experiments were carried out in 0.1 M phosphate buffer solution at pH 7.2 in the presence of 1 mM NAD^+ and 25 µM $[Cp^*Rh(bpy)Cl]^+$, under nitrogen atmosphere, at an operating potential of -0.5 V vs Ref. (H_2) with either (A) a constant solution flow rate or (B) a constant hydrogen from rate of 20 mL.min^{-1} each.

The effect of the non-humidified hydrogen flow rate in the anodic compartment was then examined in a series of experiments using increased flow rates of pure hydrogen from 1 mL.min^{-1} to 20 mL.min^{-1} at -0.5 V vs ref. (H_2). As shown by Figure 3A, higher conversion was actually allowed upon increased hydrogen flow rate. The conversion was very low with 1 mL.min^{-1} H_2 (curve a, 0.12 after 15 min), but was total within the same time period upon 20 mL.min^{-1} hydrogen (curve d). As a matter of fact, the amount of hydrogen consumed at the anode is far lower than 1 cm^3.min^{-1} after Faraday's law. Therefore, the lower performance of the cell at flow rates below 20 mL.min^{-1} is presumably due to small leakage in the hydrogen circuit and in the

flow cell, with possible maldistribution of the fuel gas in the bipolar plate channel at too low flow rates. Besides, the faradaic efficiency of NADH regeneration remains unchanged at approx. 96% for all tested hydrogen flow rates, partly owing to 100 % current efficiency for hydrogen oxidation on a GDE and because this faradaic efficiency is certainly controlled by the conditions applied in the cathodic compartment, i.e. flow, potential and concentrations. The main limitation comes from the anodic side being the amount of hydrogen that can be oxidized at the GDE to provide all electrons needed for the regeneration of NADH.

To confirm this hypothesis, the effect of the solution flow rate on the conversion was also followed with a positive effect on the conversion rate as shown in Figure 3B. Larger solution flow rates favor its uniform distribution within the porous electrode and mass transport between species, thus improving the overall conversion rate. The conversion was 0.78, with an average reaction rate of 7.08 $mmol.L^{-1}.s^{-1}$, after 15 min of electrolysis with the solution flowing at 4 $mL.min^{-1}$ (curve a); however, the conversion at the same time with a solution flow rate of 10 $mL.min^{-1}$ attained 0.93 with an average reaction rate of 8.16 $mmol.L^{-1}.s^{-1}$ (curve b). In contrast with what was observed with the effect of hydrogen flow rate, the faradaic efficiency of the reaction increased with the solution flow rate, passing from 83 % at 4 $mL.min^{-1}$ to 96 % at 20 $mL.min^{-1}$ (curve c). These data clearly show that the faradaic efficiency is also controlled by flow conditions in the cathodic compartment.

3.3. Effect of pH on NADH regeneration

The effect of pH on the NADH regeneration was studied in 0.1 M of phosphate buffer with different ratio of K_2HPO_4 (99%) and KH_2PO_4 (99%) for pH between 4 and 7.2 and upon addition of 0.1 M of tris-HCl for the pH of 9. The current variations (Figure 4A) have very similar profiles for pH 6.5, 7.2, and 9 featuring an asymptote after 15 min operation corresponding to

nearly complete conversion. However, at pH 4 the current decreases far less in absolute value than in neutral or slightly alkaline media. The conversion (Figure 4B) and the faradaic efficiency (Figure 4C), in relation with the current variations (Figure 4A), are increasing with the solution pH. In the acidic medium, the conversion attained 60% after 20 min, with a faradaic efficiency near 72 %. By contrast, full conversion was obtained within 20 min for all other pH values, whereas the faradaic efficiency increased from 87 % at pH 6.5 to 98 % at pH 9 showing the increased selectivity of the electrocatalytic reaction when proton concentration is lowered. It is also reported in the literature that NADH is unstable in acidic environment while NAD^+ is unstable in alkaline media.[51] Thus, as a compromise between stability of the molecules and acceptable faradaic efficiency, the optimal pH for NADH regeneration was taken in the range 6.5 - 7.2.

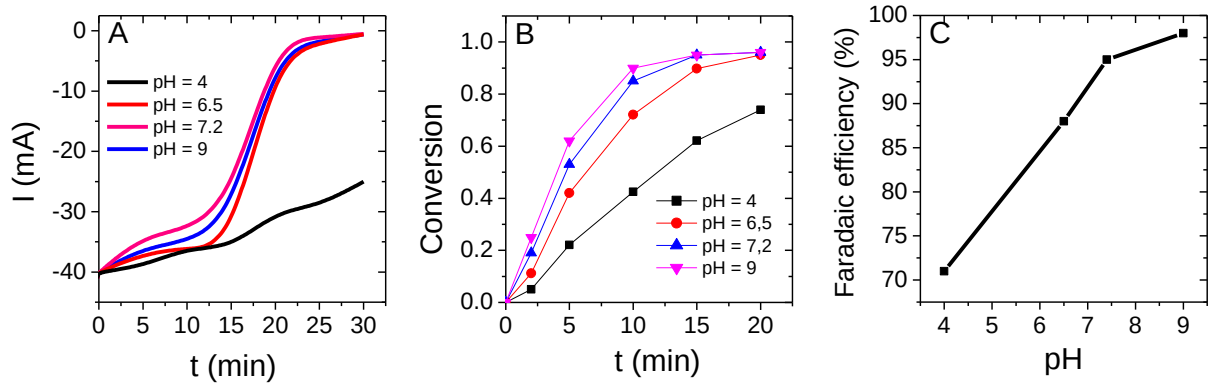

Figure 4. Influence of the solution pH on (A) the current, (B) the conversion and (C) the faradaic yield for the mediated transformation of NAD^+ to NADH. All experiments were performed in 0.1 M phosphate buffer solution in the presence of 1 mM NAD^+ and 25 µM $[Cp^*Rh(bpy)Cl]^+$ under nitrogen atmosphere with solution and hydrogen flow rates of 20 $mL.min^{-1}$ each.

3.4. Turnover number

Regeneration of NADH using the same NAD^+ over Rh concentration ratio was carried out at various concentration levels, at -0.5V vs ref. (H_2). For a [NAD^+]/[Rh] ratio of 40, as shown in Figure 5, very similar conversion rates were observed for Rh complex concentrations ranging from 12.5 to 62.5 µM, with differences in average reaction rates below 13%. For example, the average rate of the reaction using 2.5 mM NAD^+ and 62.5 µM $[Cp^*Rh(bpy)Cl]^+$ is $8.16*10^{-4}$ $mol.L^{-1}.s^{-1}$ fairly similar to the average reaction rate with 0.5 mM NAD^+ and 12.5 µM $[Cp^*Rh(bpy)Cl]^+$ ($7.8*10^{-4}$ $mol.L^{-1}.s^{-1}$). Measured in the first 5 min of the reaction, TN is in this case 370 h^{-1}, far larger than that reported in the literature, at room temperature (25 °C), for rhodium complex in solution from 0.68 to 6.3 h^{-1}. [15,52] While applying the chemical regeneration of the NADH cofactor with this rhodium complex, reduced by action of phosphite species,[53] the TN obtained was equal 21 h^{-1} using the same operational conditions of temperature and pH.

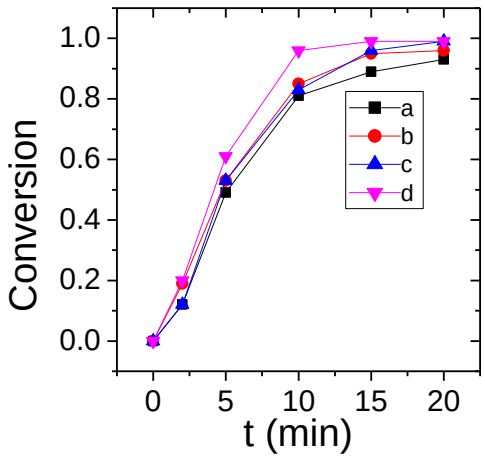

Figure 5. Studying the reduction of NAD^+ using the same ratio of NAD^+ and $[Cp^*Rh(bpy)Cl]^+$ (40) and the electrolysis potential (-0.5 V vs H_2 oxidation) using different concentrations of NAD^+ and $[Cp^*Rh(bpy)Cl]^+$: (a) 2.5 mM NAD+ and 62.5 µM $[Cp^*Rh(bpy)Cl]^+$, (b) 1.25 mM NAD^+ and 31.25 µM $[Cp^*Rh(bpy)Cl]^+$, (c) 1 mM NAD^+ and 20 µM $[Cp^*Rh(bpy)Cl]^+$, (d) 0.5 mM NAD^+ and 12.5 µM $[Cp^*Rh(bpy)Cl]^+$. All experiments were performed in

0.1 M phosphate buffer solution at pH 7.2 under nitrogen atmosphere with solution and hydrogen flow rates of 20 $mL.min^{-1}$ each.

In such conditions, the conversion is total in all studied cases and the ratio between $[NAD^+]$ and $[Cp^*Rh(bpy)Cl]^+$ corresponds to the TTN. This TTN can only be increased here if the regenerated cofactor is consumed continuously by an enzymatic reaction, a development briefly examined in this study and described in the next section with lactate dehydrogenase as example. Enzymatic systems applied continuously with the electrochemical regeneration of the NADH depend on the amount of enzymes used, in relation to the quantity of substrate to be converted, which rules the time required for given bioconversion. For that purpose, it was important to evaluate the stability of the regenerated NADH with time. Results showed that 98 % of the regenerated NADH after 72 hours were still stable and active as shown in Figure S4 of the Supporting Information.

3.5. Application of regenerated NADH in an enzymatic reaction

After having determined the optimal parameters for the efficient regeneration of NADH in the flow electrochemical reactor, integrating an enzymatic reaction in the process was attempted to validate the production of the active form of the NADH cofactor regenerated in the above mediated redox process. This is indeed important for the practical application of such bioelectrocatalytic system[24] and for the evaluation of its possible use in the production of fine chemicals as expected from biocatalysis in biotechnology.[41] For this purpose, Lactate dehydrogenase was used here since it is a widely available NAD-dependent enzyme, whose substrate and products can be easily analyzed. The first step in this work was to demonstrate the stability and the selectivity of LDH enzymes immobilized on the chosen support in the presence of dissolved rhodium complex and NAD^+/NADH species (reported in Figure S5 in Supporting

Information). The second step was to prove that NADH was regenerated with a high purity and exhibiting a high activity towards the bioconversion of pyruvate to lactate in comparison to the commercial one (reported in Figures S6 to S9 in Supporting Information). The third step was the application of the regenerated NADH for the conversion of pyruvate to lactate in the presence of the rhodium complex. It was assumed that the bioconversion occurs at the surface of the LDH-MWCNT-CP. For this reason, it was important to evaluate the optimal amount of LDH that has to be added on MWCNT. 500 units ~~of~~ LDH were found sufficient (> 200 U/cm² CP-MWCNT) for the efficient bioconversion of pyruvate to lactate, as reported in Fig. S10 of the Supporting Information). In a previous report from the literature, 1400 U ~~of~~ LDH were added to a 50 mL solution containing 2 mM NAD^+ and 20 mM pyruvate.[15]

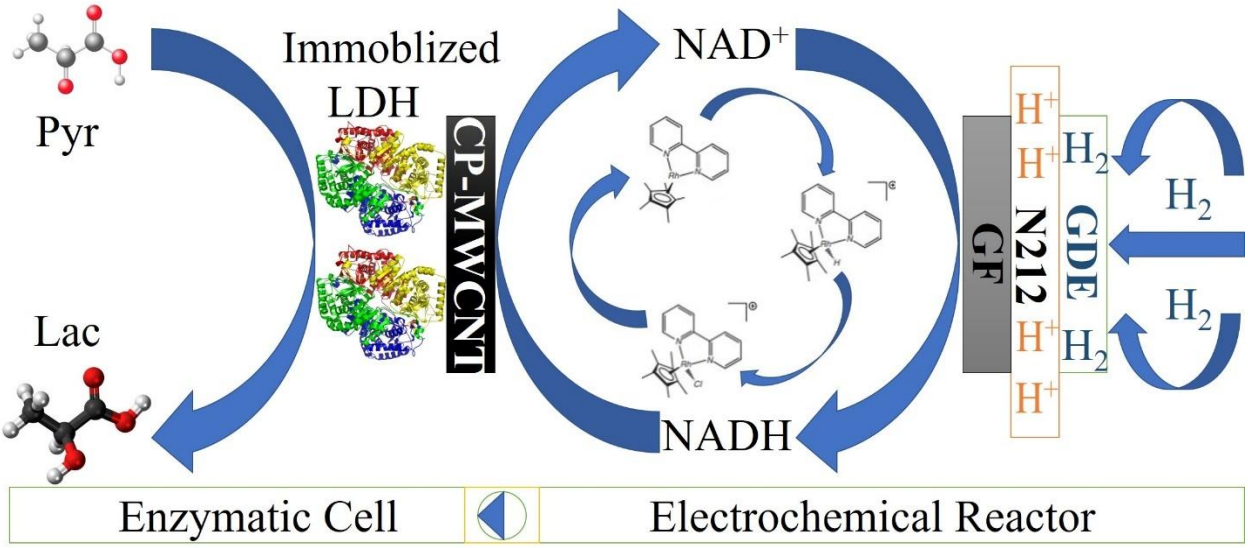

Scheme 3. Schematic representation of the electrochemical reactor in series with the enzymatic cell including Rh-mediated electrochemical and enzymatic reactions with the LDH-MWCNT-CP system.

Scheme 3 represents the electrochemical reactor in series with the enzymatic cell in the recirculation loop, with the rhodium complex in solution. 40 mL 0.1 M PBS solution at 7.2, containing 0.5 mM NADH, 12.5 µM $[Cp^*Rh(bpy)Cl]^+$, and 25 mM pyruvate, was circulated in

the electrochemical reactor, whose cathode was operated at -0.5 V vs ref. (H_2). The carbon-based support of the enzymatic cell was loaded with 500 units LDH. The experiment was carried out under nitrogen degassing, with 20 $mL.min^{-1}$ hydrogen and solution flows (as determined above). For the sake of comparison, another test was made without the enzymatic cell, and with 0.5 mM NAD^+ instead of NADH in the solution. As shown in Figure 6A without the enzymatic cell (curve a), the cathodic current decreased gradually from 37 to 30 mA (abs. value), then decayed more rapidly after 15 min, corresponding to the large conversion extent of NAD^+ (over 85%). However, with the enzymatic cell in series (curve b), a fairly stable current in the order of 21 mA (approx. 1.3 $mA.cm^{-2}$) was observed, revealing indirectly the activity of the rhodium complex toward the regeneration of the NADH consumed in the enzymatic reaction. Contrary to what was observed with test (a), the combined system was operated with balanced NADH enzymatic consumption and electrode regeneration over the 30 min period shown in Fig. 6A. The current remained at a comparable level during the combined electro-enzymatic test carried out for 5 hours, with a current regularly decreasing from 21 mA to 16 mA after 5 hours electrolysis (Fig. 6B).

The concentration of the enzymatic cofactor decreased rapidly in the 10 first minutes of the run (Fig. 6C) to less than 0.1 mM, due to its quantitative LDH-catalyzed consumption. In the meanwhile, the lactate concentration raised to 0.56 mM, corresponding to approx.1.12 times of the initial NADH concentration of the NADH cofactor, *i.e.* with little significant NADH regeneration. Afterward, the NADH concentration slowly increased, attaining 0.17 M after 4 hours, whereas pyruvate was efficiently converted to lactate (Fig. 6D), with equilibrated constant rates between electrochemical and enzymatic processes. In the last hour, the lower pyruvate concentration rendered the enzymatic reaction slower, resulting in increased NADH

concentration (0.41 mM after 5 hours). Conversion was nearly total after 5 hours, with a 24.7 mM lactate final concentration, corresponding approximately to 50-times of the initial NADH concentration. The faradaic efficiency was higher than 90% during the first hours of reaction, but decreased abruptly during the last hour to 61 %, *i.e.* below ~~than~~ that obtained without enzymes (96 %). Apparently, the decrease in NAD^+concentration in the flow reactor when NADH was not consumed anymore by LDH (because of the full conversion of pyruvate to lactate), provided more opportunities for side electrochemical reactions, e.g. reduction of oxygen traces or hydrogen evolution.

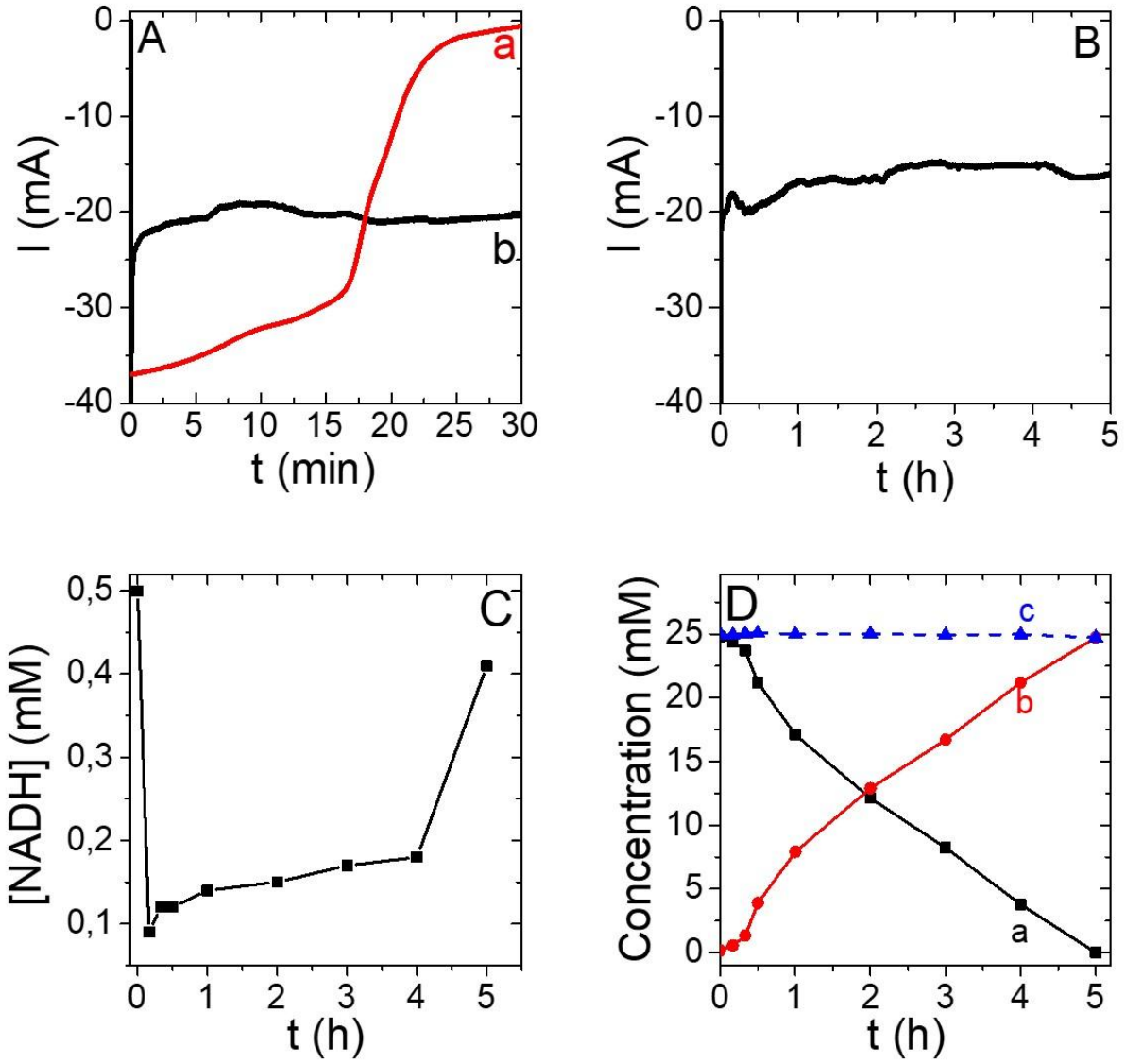

Figure 6. (A) Current recorded after the addition of 25 mM pyruvate recorded using 12.5 µM $[Cp^*Rh(bpy)Cl]^+$ in solution (a) without the enzymatic cell and with 0.5 mM of NAD^+ and (b) with the enzymatic cell. (B) Current, and (C) NADH evolution recorded with time in test (b). (D) Time variations of the concentrations of (a) pyruvate, (b) lactate, and (c) the sum of pyruvate and lactate, as determined by HPLC. Enzymatic reaction (Figures 6A (b), 6B, 6C, and 6D) was carried out in 0.1 M PBS solution at pH 7.2, with 0.5 mM NADH and 12.5 µM $[Cp^*Rh(bpy)Cl]^+$

under nitrogen atmosphere, H_2 and solution flow rates at 20 mL.min^{-1} with 500 units of LDH immobilized on MWCNT-CP. In both tests, the cathode potential was at -0.5 V. vs ref. (H_2).

A total turnover number of more than 2000 was obtained for the rhodium complex after 5 h, which is the highest value ever obtained with rhodium complex in solution, compared with those in former electroenzymatic synthesis tests for the bioconversion at room temperature, reported between 55 and 214.[54],[55] Without the application of an enzymatic reaction, the highest TTN for the rhodium complex applied in the electrochemical regeneration of the NAD(P)H cofactor was 400.[56] In addition, the TN in the period from 1 to 4 hour with enzymes was near 300 h^{-1}, in the same order of magnitude but slightly lower than the value of 370 h^{-1} obtained without enzymes in the presence of a higher concentration of NAD^+ (2.5 mM reported in Figure 5 versus 0.5 mM in Figure 6); TTN obtained for the enzymatic reaction was equal to $6.3*10^6$ showing the good stability of the flow device combining the electrochemical reactor and the enzymatic cell. No conversion was observed in the absence of NADH (Figure S11 of the Supporting Information). The lactate produced by the redox flow bioreactor displayed a very good purity, over 99% as determined by 1H NMR (Figures S12-S13 of the Supporting Information).

4. Conclusion

In summary, we have demonstrated the full potential of a bioelectrochemical reactor for the regeneration of NADH that couples efficiently the oxidation of hydrogen to the reduction of NAD^+ mediated by a rhodium complex: high activity with a TN of 370 h^{-1} for TTN value near 40 was shown.

The efficient regeneration of NADH featured with a complete conversion and with a high faradaic yield can be reached by fixing different parameters for the used reactor at their optimal

values: hydrogen and solution flow rates (20 $mL.min^{-1}$), NAD^+ to $[Cp^*Rh(bpy)Cl]^+$ concentration ratio (40), pH (close to neutrality, to avoid NADH and NAD^+ degradation).

Based on these optimized parameters for the regeneration of the NADH cofactor, adding an enzymatic reaction for the bioconversion of pyruvate to lactate by the LDH-CP-MWCNT showed its high efficiency and stability with a high TTN for the cofactor electrochemical regeneration and the enzymatic reaction of 2000 and $6.3*10^6$, respectively. In addition, no deactivation of both the rhodium complex and the LDH was observed here (a possible deactivation is reported in the literature[55]).

The electrochemical reactor and the enzymatic cell, presented in Schemes 1 and 2 respectively, are in principle scalable. While the performances regarding TN and TTN of the rhodium catalyst in solution are larger than those reported in the literature, one must be aware that TN and TTN for the catalyst are still lower than enzymatic based electrogeneration associated to surface immobilization.[11,57] Moreover, TTN for the cofactor in the electroenzymatic synthesis remain largely lower than the most recent achievements with closely confined enzymatic catalyst also immobilized on the surface of porous electrodes.[58] As a perspective, the immobilization of the rhodium complex allowing much higher TTN (up to 12 000)[26,59] has to be applied for this flow reaction and associated more closely with the enzymatic reaction in order to promote the best cycling of both the catalyst and the enzymatic cofactor and potentially easier purification of the synthesized molecules. In this way, one could promote the application of redox flow technologies in quite relevant industrial topic: dehydrogenases allow for the development of blocks of chiral synthesis comprising various functions e.g. alcohols, hydroxy acids, aldehydes and ketones having a large interest in cosmetics, food, and pharmaceutical industries.[5] Besides, lactate production from lactate dehydrogenase, the illustrative example ~~that is~~ considered in this

study, is widely used in various applications e.g. food, cosmetics, pharmaceutical, and chemical industries[6],[7]

Acknowledgement. We gratefully acknowledge CNRS for funding of the project NADP/H_2. We also thank Neus Vilà (LCPME) for help in the rhodium complex synthesis, Steve Pontvianne and Xavier Framboisier (LRGP) for development of the HPLC analytical method and Olivier Fabre at the LCPM laboratory for the NMR measurements.

Supporting Information. Cyclic voltammetry of electrochemical reduction of NAD^+ in the presence of various concentrations of $[Cp^*Rh(bpy)Cl]^+$; an example of non-complete conversion; validation of the flow enzymatic reactor with short discussion of the reported data, illustration of optimal LDH quantity for the bioconversion of pyruvate, control experiments regarding NADH regeneration and stability, 1H NMR analysis of NADH and lactate.

References

[1] L. Sorci, O. Kurnasov, D. A. Rodionov, A. L. Osterman, in *Compr. Nat. Prod. II Chem. Biol.*, Elsevier, **2010**, pp. 213–257.

[2] H. K. Chenault, G. M. Whitesides, *Appl. Biochem. Biotechnol.* **1987**, *14*, 147–197.

[3] R. Jerôme, Contineous Regeneration of the NADH Cofactor Catalyzed by Formate Dehydrogenase in a Filter Press Reactor, Université Toulouse III-Paul Sabatier, **2011**.

[4] R. Devaux-Basseguy, A. Bergel, M. Comtat, *Enzyme Microb. Technol.* **1997**, *20*, 248–

258.

[5] R. Patel, M. Kula, U. Kragl, *Stereoselective Biocatal.* **2000**, *13*, 839–866.

[6] Y. J. Wee, J. N. Kim, H. W. Ryu, *Food Technol. Biotechnol.* **2006**, *44*, 163–172.

[7] E. T. H. Vink, K. R. Rábago, D. A. Glassner, P. R. Gruber, *Polym. Degrad. Stab.* **2003**, *80*, 403–419.

[8] L. Zhang, M. Etienne, N. Vilà, A. Walcarius, in *Funct. Electrodes Enzym. Microb. Electrochem. Syst.* (Eds.: N. Brun, V. Flexer), World Scientific, **2017**, pp. 215–271.

[9] J. B. Jones, D. W. Sneddon, W. Higgins, A. J. Lewis, *J. Chem. Soc. Chem. Commun.* **1972**, 856–857.

[10] G. T. Höfler, E. Fernández-Fueyo, M. Pesic, S. H. Younes, E. G. Choi, Y. H. Kim, V. B. Urlacher, I. W. C. E. Arends, F. Hollmann, *ChemBioChem* **2018**, *19*, 2344–2347.

[11] B. Siritanaratkul, C. F. Megarity, T. G. Roberts, T. O. M. Samuels, M. Winkler, J. H. Warner, T. Happe, F. A. Armstrong, *Chem. Sci.* **2017**, *8*, 4579–4586.

[12] C. Virto, I. Svensson, P. Adlercreutz, B. Mattiasson, *Biotechnol. Lett.* **1995**, *17*, 877–882.

[13] G. C. Xu, H. L. Yu, Y. P. Shang, J. H. Xu, *RSC Adv.* **2015**, *5*, 22703–22711.

[14] K. D. Kulbe, M. W. Howaldt, K. Schmidt, T. R. Röthig, H. Chmiel, *Ann. N. Y. Acad. Sci.* **1990**, *613*, 820–826.

[15] R. Ruppert, S. Herrmann, E. Steckhan, *Tetrahedron Lett.* **1987**, *28*, 6583–6586.

[16] E. Siu, K. Won, C. B. Park, *Biotechnol. Prog.* **2007**, *23*, 293–296.

[17] B. Cheng, L. Wan, F. A. Armstrong, *ChemElectroChem* **2020**, *7*, 4672–4678.

[18] H. K. Chenault, E. S. Simon, G. M. Whitesides, *Biotechnol. Genet. Eng. Rev.* **1988**, *6*, 221–270.

[19] H. Zhao, W. A. van der Donk, *Curr. Opin. Biotechnol.* **2003**, *14*, 583–589.

[20] C. Kane, Design and Production of Electrochemical Microreactors: Application to the Electroenzymatic Regeneration of NADH and Potentialities in Synthesis, University Toulouse 3, **2005**.

[21] J. Cantet, Process for the Regeneration of the NADH Cofactor by the Simultaneous Use of an Electrode and a Hydrogenase, University Toulouse 3, **1992**.

[22] S. Fukuzumi, Y.-M. Lee, W. Nam, *J. Inorg. Biochem.* **2019**, *199*, 110777.

[23] C. F. Megarity, B. Siritanaratkul, B. Cheng, G. Morello, L. Wan, A. J. Sills, R. S. Heath, N. J. Turner, F. A. Armstrong, *ChemCatChem* **2019**, *11*, 5662–5670.

[24] A. Walcarius, R. Nasraoui, Z. Wang, F. Qu, V. Urbanova, M. Etienne, M. Göllü, A. S. Demir, J. Gajdzik, R. Hempelmann, *Bioelectrochem.* **2011**, *82*, 46–54.

[25] H. Jaegfeldt, *J. Electroanal. Chem. Interfacial Electrochem.* **1981**, *128*, 355–370.

[26] L. Zhang, M. Etienne, N. Vilà, T. X. H. Le, G.-W. Kohring, A. Walcarius, *ChemCatChem* **2018**, *10*, 4067–4073.

[27] B. Tan, D. P. Hickey, R. D. Milton, F. Giroud, S. D. Minteer, *J. Electrochem. Soc.* **2015**, *162*, H102–H107.

[28] E. Steckhan, S. Herrmann, R. Ruppert, E. Dietz, M. Frede, E. Spika, *Organometallics* **1991**, *10*, 1568–1577.

[29] H. C. Lo Leiva, C., Buriez, O., Kerr, J. B., Olmstead, M. M., & Fish, R. H., *Bioorganometallic Chem.* **2001**.

[30] A. Goršek, P. Glavič, *Chem. Eng. Res. Des.* **1997**, *75*, 709–717.

[31] T. Noël, Y. Cao, G. Laudadio, *Acc. Chem. Res.* **2019**, *52*, 2858–2869.

[32] H. Löwe, M. Kuepper, A. Ziogas, in *Proceeding Third Int. Conf. Microreact. Technol. (IMRET 3)*, Springer Science & Business Media, **2000**, p. 136.

[33] J. Britton, S. Majumdar, G. A. Weiss, *Chem. Soc. Rev.* **2018**, *47*, 5891–5918.

[34] R. Porta, M. Benaglia, A. Puglisi, *Org. Process Res. Dev.* **2016**, *20*, 2–25.

[35] M. Wesselmark, B. Wickman, C. Lagergren, G. Lindbergh, *Electrochem. commun.* **2010**, *12*, 1585–1588.

[36] I. Lozano, N. Casillas, C. P. de León, F. C. Walsh, P. Herrasti, *J. Electrochem. Soc.* **2017**, *164*, D184.

[37] J. W. Ager, A. A. Lapkin, *Science* **2018**, *360*, 707–708.

[38] M. Varničić, T. Vidaković-Koch, K. Sundmacher, *Electrochim. Acta* **2015**, *174*, 480–487.

[39] A. E. W. Horst, K.-M. Mangold, D. Holtmann, *Biotechnol. Bioeng.* **2016**, *113*, 260–267.

[40] I. Mazurenko, M. Etienne, G. W. Kohring, F. Lapicque, A. Walcarius, *Electrochim. Acta* **2016**, *199*, 342–348.

[41] M. T. Reetz, *J. Am. Chem. Soc.* **2013**, *135*, 12480–12496.

[42] R. Agudo, G. D. Roiban, M. T. Reetz, *J. Am. Chem. Soc.* **2013**, *135*, 1665–1668.

[43] R. A. Sheldon, S. van Pelt, *Chem. Soc. Rev.* **2013**, *42*, 6223–6235.

[44] J. Quinson, R. Hidalgo, P. A. Ash, F. Dillon, N. Grobert, K. A. Vincent, *Faraday Discuss.* **2014**, *172*, 473–496.

[45] U. Koelle, A. D. Ryabov, *Mendeleev Commun.* **1995**, *5*, 187–189.

[46] V. Sivasankar, P. Mylsamy, K. Omine, *Microbial Fuel Cell Technology for Bioelectricity*, Springer International Publishing, Cham, **2018**.

[47] L. Hussein, G. Urban, M. Krüger, *Phys. Chem. Chem. Phys.* **2011**, *13*, 5831–5839.

[48] E. V LaBelle, H. D. May, *Front. Microbiol.* **2017**, *8*, 756.

[49] L. Gorton, E. Domínguez, E. Dominguez, in *Encycl. Electrochem.*, Wiley-VCH Verlag GmbH & Co. KGaA, Weinheim, Germany, **2007**, pp. 67–143.

[50] S. Goswami, S. Klaus, J. Benziger, *Langmuir* **2008**, *24*, 8627–8633.

[51] L. Rover Júnior, J. C. Fernandes, G. de Oliveira Neto, L. T. Kubota, E. Katekawa, S. H. Serrano, *Anal. Biochem.* **1998**, *260*, 50–55.

[52] S. Lee, H. Choe, D. H. Cho, S. H. Yoon, K. Won, Y. H. Kim, *J. Electrochem. Soc.* **2016**, *163*, G50–G52.

[53] M. M. Grau, M. Poizat, I. W. C. E. Arends, F. Hollmann, *Appl. Organomet. Chem.* **2010**, *24*, 380–385.

[54] F. Hildebrand, S. Lütz, *Tetrahedron Asymmetry* **2007**, *18*, 1187–1193.

[55] F. Hildebrand, S. Lütz, *Chem. Eur. J.* **2009**, *15*, 4998–5001.

[56] K. Vuorilehto, S. Lütz, C. Wandrey, *Bioelectrochemistry* **2004**, *65*, 1–7.

[57] M. Yuan, M. J. Kummer, R. D. Milton, T. Quah, S. D. Minteer, *ACS Catal.* **2019**, 5486–5495.

[58] C. F. Megarity, B. Siritanaratkul, R. S. Heath, L. Wan, G. Morello, S. R. FitzPatrick, R. L. Booth, A. J. Sills, A. W. Robertson, J. H. Warner, N. J. Turner, F. A. Armstrong, *Angew. Chem. Int. Ed.* **2019**, *58*, 4948–4952.

[59] L. Zhang, N. Vilà, G. W. Kohring, A. Walcarius, M. Etienne, *ACS Catal.* **2017**, *7*, 4386–4394.

[60] S. Kochius, A. O. Magnusson, F. Hollmann, J. Schrader, D. Holtmann, *Appl. Microbiol. Biotechnol.* **2012**, *93*, 2251–2264.